TISSUE ENGINEERING: Part A
Volume 26, Numbers 3 and 4, 2020

DOI: 10.1089/ten.tea.2019.0087

termis
Tissue Engineering
& Regenerative Medicine
International Society

ORIGINAL ARTICLE

A Comparison of Ovine Facial and Limb Muscle as a Primary Cell Source for Engineered Skeletal Muscle

Brittany L. Rodriguez, MSE,[1] Matthew H. Nguyen,[2] Rachel E. Armstrong, BS,[2] Emmanuel E. Vega-Soto, BS,[2] Phillip M. Polkowski,[2] and Lisa M. Larkin, PhD[1,2]

Volumetric muscle loss (VML) contributes to the number of soft tissue injuries that necessitate reconstructive surgery, but treatment options are often limited by tissue availability and donor site morbidity. To combat these issues, our laboratory has developed scaffold-free tissue-engineered skeletal muscle units (SMUs) as a novel treatment for VML injuries. Recently, we have begun experiments addressing VML in facial muscle, and the optimal starting cell population for engineered skeletal muscle tissue for this application may not be cells derived from hindlimb muscles due to reported heterogeneity of cell populations. Thus, the purpose of this study was to compare SMUs fabricated from both craniofacial and hindlimb sources to determine which cell source is best suited for the engineering of skeletal muscle. Herein, we assessed the development, structure, and function of SMUs derived from four muscle sources, including two hindlimb muscles (i.e., soleus and semimembranosus [SM]) and two craniofacial muscles (i.e., zygomaticus major and masseter). Overall, the zygomaticus major exhibited the least efficient digestion, and SMUs fabricated from this muscle exhibited the least aligned myosin heavy chain staining and consequently, the lowest average force production. Conversely, the SM muscle exhibited the most efficient digestion and the highest number of myotubes/mm^2; however, the SM, masseter, and soleus groups were roughly equivalent in terms of force production and histological structure.

Keywords: muscle-derived progenitor cells, satellite cell, skeletal muscle, cell inhomogeneity

Impact Statement

An empirical comparison of the development, structure, and function of engineered skeletal muscle tissue fabricated from different muscles, including both craniofacial and hindlimb sources, will not only provide insight into innate regenerative mechanisms of skeletal muscle but also will give our team and other researchers the information necessary to determine which cell sources are best suited for the skeletal muscle tissue engineering.

Introduction

Maxillofacial surgery is the third most common reconstructive procedure performed in the United States. In 2017, over 200,000 reconstructive maxillofacial surgeries were conducted to repair facial disfigurements, some of which were performed to treat volumetric muscle loss (VML).[1] VML, which is defined as the degenerative, traumatic, or surgical loss of skeletal muscle, contributes to the prevalence of facial deformities and to the number of soft tissue injuries that necessitate reconstructive surgery.[2,3] Skeletal muscle inherently has a high regenerative capacity in response to injury,[4,5] but this innate capacity is overwhelmed in the case of VML. VML is characterized by a significant impairment of physical function and, as a result, usually necessitates surgical intervention.[6] Surgical intervention includes the transplantation of muscle flaps and grafts, which are limited by tissue availability and donor site morbidity, as well as the implantation of fillers and prostheses, which are limited by suboptimal integration of the material and sustained inflammatory response.[7,8] Furthermore, these treatment options do not always fully restore function and often fail to produce adequate levels of patient satisfaction.[9]

Research in tissue engineering and regenerative medicine has aimed to address the caveats of traditional surgical approaches. A living tissue-engineered muscle construct has the

[1]Biomedical Engineering, University of Michigan, Ann Arbor, Michigan.
[2]Department of Molecular and Integrative Physiology, University of Michigan, Ann Arbor, Michigan.

ability to restore muscle function, donate new muscle fibers to the repair site, recruit native regenerative cells, and integrate with native tissue, while addressing the issue of morbidity associated with current surgical treatments.[10,11] However, because the source of muscle progenitor cells for tissue engineering applications is traditionally hindlimb muscle, a potential obstacle to the engineering of facial muscle specifically is the distinct difference in developmental origin between trunk and limb muscle and craniofacial muscle. This difference is related to variations in phenotype between cell populations, including satellite cells.[12–15] The difference in developmental origin between facial and limb muscle prompts the question as to whether the difference in cell populations between these sources affects their ability to form engineered muscle tissues *in vitro*.

Studies have shown that satellite cells derived from craniofacial muscle exhibit differences in regenerative capacity, satellite cell density, and gene expression compared to trunk and limb satellite cells.[13,14,16] What has not been elucidated is whether these differences would affect the characteristics of the muscle constructs they produce. Furthermore, there is evidence to suggest that developmental origin alone cannot account for the heterogeneity of satellite cell populations, and thus their potential use in tissue engineering applications.[12,13] For example, satellite cells isolated from multiple hindlimb muscles exhibit different regenerative rates when transplanted into an identical host environment.[16] Thus, properties of satellite cell populations appear to exist as a continuum with a range of proliferative and regenerative capacities, cell densities, and differentiation timelines,[12–14] so the choice of the optimal cell source for the engineering of skeletal muscle for repair of facial VML necessitates an empirical comparison of cell populations derived from various muscle sources.

Currently, skeletal muscle tissue engineering is almost exclusively performed using muscle progenitor cell populations derived from limb muscles. This includes work from our laboratory, which, to date, has solely involved cell populations derived from hindlimb muscles with the intention of treating VML in other hindlimb muscles.[10,17,18] Recently, we have begun experiments addressing VML in facial muscle, and because of the apparent heterogeneity of satellite cell populations, we find it appropriate to explore the potential difference in craniofacial versus hindlimb muscle-derived cell populations. Thus, the purpose of this study is to compare the proliferative capacity and differentiation capabilities of cell populations derived from both craniofacial and hindlimb muscle sources. This will not only provide insight into innate regenerative mechanisms of varied skeletal muscle sources but will also give our team the information necessary to determine which cell source is best suited for skeletal muscle tissue engineering.

Specifically, in this study, we assessed the development, structure, and function of our laboratory's skeletal muscle units (SMUs) derived from four muscle sources, including two hindlimb muscles (i.e., soleus and semimembranosus [SM]) and two craniofacial muscles (i.e., zygomaticus major and masseter). The soleus muscle is a postural muscle located in the hindlimb and is primarily composed of type I fibers in humans.[19] Due to the higher satellite cell density in the muscle, the soleus muscle has been the muscle source of choice for our previous rat SMU studies.[10,17,18] The SM is also a hindlimb muscle and is commonly used in ovine satellite cell studies[20–22] due to the reduced amount of connective tissue and the relative ease of access compared to the soleus. In humans, the SM is relatively evenly divided between type I and type II fibers.[23] The masseter is a mastication muscle located in the jaw and is primarily composed of type I fibers in humans.[24,25] The zygomaticus major is a superficial muscle used in facial expression and is primarily composed of type II fibers in humans.[25,26]

We expect satellite cell density to correlate to the fiber type composition of the muscle, with the muscles predominantly composed of type I fibers having a higher satellite cell density, as has been observed previously.[27] Furthermore, it is likely that the muscles with the highest myogenic cell densities will have the greatest myogenic potential, and thus produce SMUs with the greatest myotube density, most advanced structure, and greatest force production. However, there are other aspects to consider in addition to myogenic potential. For example, it is likely that muscles with more connective tissue will yield a higher number of fibroblasts during enzymatic digestion, which is not ideal for our construct fabrication. Thus, we hypothesized that muscles with higher amounts of visible connective tissue will produce constructs with lower force production and lower myotube density compared to other muscle sources.

Materials and Methods

Experimental design

To elucidate the effects of the muscle progenitor cell source, we cultured sheep muscle isolates from four muscle sources (i.e., soleus, SM, zygomaticus major, and masseter muscles) and evaluated the SMU development throughout the fabrication process. Specifically, we evaluated the development (myogenesis), structure (histology), and functional outcomes (biomechanics) of the resultant SMUs. The experimental timeline is summarized in Figure 1 and was identical for each group.

Muscle biopsy collection

All animal care procedures followed *The Guide for Care and Use of Laboratory Animals*,[28] according to a protocol approved by the University's Institutional Animal Care & Use Committee. Polypay sheep between 10 and 13 months of age (Oswalt Farms, Vicksburg, MI) were anesthetized through the administration of intravenous propofol (8 mg/kg) and gaseous isoflurane at concentrations between 2% and 5% to maintain a deep plane of anesthesia. Midsubstance biopsies from the SM, soleus, masseter, and zygomaticus major muscles of sheep were collected under aseptic conditions. After tissue dissection, animals were subsequently euthanized through the administration of a lethal dose of Beuthansia-D Special (195 mg/kg) and subsequent bilateral pneumothorax. The biopsies were transported to the laboratory in chilled Dulbecco's Phosphate Buffered Saline (DPBS) supplemented with 2% antibiotic-antimycotic (Cat. No. 15240-062; Gibco).

Cell isolation

Muscle biopsies between 0.8 and 0.9 g were sanitized in 70% ethanol and finely minced with a razor blade. The minced muscle was placed under ultraviolet light for 5 min

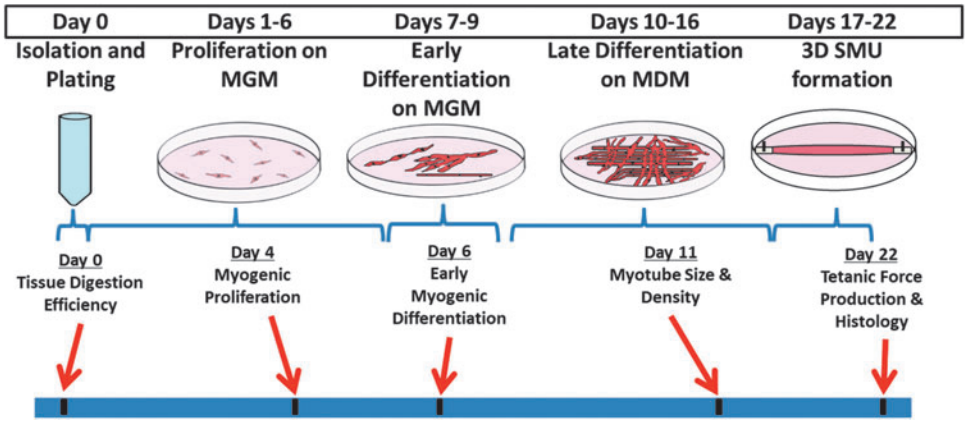

FIG. 1. Summary of experimental design. To compare constructs fabricated from different muscle sources, we cultured sheep muscle isolates and evaluated the development, structure, and function of our SMUs at different time points throughout the fabrication process. These assessments were completed on each of four experimental groups: zygomaticus major, masseter, soleus, and SM muscle sources. MDM, muscle differentiation medium; MGM, muscle growth medium; SM, semimembranosus; SMU, skeletal muscle unit.

and subsequently added to a digestion solution composed of 2.3 mg/mL dispase (Cat. No. 17105-041; Thermo Fisher) and 0.3 mg/mL collagenase type IV (Cat. No. 17104-019; Thermo Fisher). The digestion was incubated for a total of 2.25 h at 37°C with constant agitation. The resulting suspension was then filtered through a 100 µm mesh filter (Cat. No. 22-363-549; Fisher Scientific) followed by filtration through a 40 µm mesh filter (Cat. No. 22-363-547; Fisher Scientific) and centrifuged. The supernatant was discarded, and the cells were resuspended in muscle growth medium as described previously.[10,17,29]

Digestion efficiency

After enzymatic digestion of the muscle biopsies, the undigested tissue captured by the 100 µm mesh filter was blotted and weighed to provide insight into the digestion efficiency of each type of muscle. In addition, cell counts were taken from the isolation's resultant cell suspension and normalized to the mass of muscle digested to provide insight into the cell yield per unit mass of muscle. An aliquot of the cell suspension was stained with acridine orange and propidium iodide and counted using a LUNA-FL Cell Counter (Logos Biosystems, Annandale, VA).

Characterization of starting cell populations

After completion of the cell isolation, cells that were not immediately seeded onto tissue culture plastic were cryogenically preserved in media containing 10% dimethyl sulfoxide. To obtain samples for immunocytochemistry, the cells were thawed and diluted in DBPS to a concentration of $1–2 \times 10^6$ cells/mL. Two hundred microliter aliquots of the resultant cell suspension were adhered to glass microscope slides by way of the cytospin technique. The samples were then immunocytochemically stained for Pax7 (Cat. No. Pax7c; DHSB) and MyoD (Cat. No. ab16148; Abcam) to identify satellite cells and other myogenic cells, as well as vimentin (Cat. No. ab45939; Abcam) to identify mesenchymal cells, including fibroblasts. DAPI was used to identify total cell nuclei (Cat. No. P36935; Thermo Fisher). A combination of antigen retrieval and the use of a Tyramide SuperBoost Kit (Cat. No. B40912; Thermo Fisher) was used to identify Pax7 and MyoD.

Briefly, the samples were fixed in 4% paraformaldehyde, washed in DPBS, and then treated with the $100 \times H_2O_2$ solution according to the SuperBoost kit instructions. The samples then underwent an antigen retrieval step in which the samples were submerged in 10 mM citrate buffer, maintained at 92°C for 11 min, and then allowed to cool. The samples were then blocked with 10% goat serum in DPBS for 1 h. Primary antibodies for Pax7, MyoD, and vimentin were diluted in 10% goat serum blocking solution at a ratio of 1:100. The samples were incubated with the primary antibody at 4°C overnight. The following day, the slides were washed and then incubated with goat anti-mouse poly horseradish peroxidase antibody according to SuperBoost kit instructions for 1 h. The samples were then washed in DPBS and subsequently treated with tyramide working solution for 10 min, followed by treatment with Stop Reagent for 3 min, according to SuperBoost kit instructions. The samples were then washed in DPBS and subsequently incubated with a goat anti-rabbit secondary antibody for 1 h. The samples were then washed and mounted with a coverslipping medium containing DAPI.

The entirety of the cytospin samples was imaged automatically at 10× magnification on a Zeiss Apotome microscope set to capture a 10% image overlap. Fully stitched images were analyzed using ImageJ/Fiji. The total number of DAPI-stained nuclei was enumerated using the Analyze Particles function in ImageJ/Fiji. Positive staining for Pax7/MyoD that colocalized with nuclei was enumerated to determine the percentage of myogenic cells relative to total cells. We also enumerated the number of cells expressing vimentin, and the number of cells expressing both vimentin and Pax7/MyoD in the same manner.

Proliferative capacity

To assess the cells' proliferative capacities, muscle cell isolates were seeded onto 35 mm laminin-coated Sylgard

plates at a density of 200,000 cells per plate. Plate preparation was completed as described previously.[10,17] Three days after initial seeding, the cells were treated with BrdU labeling reagent (Cat. No. 000103; Thermo Fisher) at a concentration of 1:100 to identify proliferating cells. On day 4, 24 h after BrdU treatment, the plates were fixed in −20°C methanol for 10 min. Immunostaining for BrdU (Cat. No. ab92837; Abcam) and MyoD (Cat. No. ab16148; Abcam), a myogenic transcription factor that identifies myogenic proliferating cells, allowed us to determine the number of $MyoD^+$ cells and the number of $BrdU^+$ cells per unit area. The plates were imaged and the cells with positive staining were enumerated.

Early differentiation

To assess the cells' degrees of early differentiation, muscle cell isolates were seeded onto 35 mm laminin-coated Sylgard plates at a density of 200,000 cells per plate. Six days after initial seeding, the plates were fixed in −20°C methanol for 10 min. Immunostaining for myogenin (Cat. No. ab103924; Abcam), a myogenic transcription factor present in differentiating myogenic cells, was used to determine the number of differentiating myogenic cells per unit area. The plates were imaged and the cells with positive staining were enumerated.

Late differentiation

To evaluate late differentiation, we measured myotube size and density. Muscle cell isolates were plated on 60 mm laminin-coated Sylgard plates at a seeding density of 600k cells per plate. The cells were allowed to expand in culture until day 7, at which point the culture media were switched to promote further differentiation, as described previously.[10,17] On day 11, six representative images were taken of monolayers using light microscopy. These images were used to evaluate myotube size (diameter) and density using the ImageJ software package. Myotube density is defined as the number of myotubes per unit area.

Function

On day 10, minutien pins were anchored to the developing monolayers described in the Late Differentiation section. The monolayers were scored around the outside edges 17 days after initial seeding to promote delamination around the anchors. Over the course of days 18–21, the monolayers fully rolled up around the pins to produce cylindrical 3D constructs. On day 22, a minimum of 24 h after 3D construct formation, tetanic isometric force production was measured to evaluate functionality, as described previously.[10,17,30] Briefly, the pin anchoring one end of the construct was adhered to an optical force transducer and released from the Sylgard. Platinum wire electrodes were placed on either side of the construct for electrical field stimulation. Throughout the duration of testing, the temperature and hydration of the construct in media heated to 37°C. Tetanic isometric forces were elicited with a 1 s square wave stimulus with a 5 ms pulse and 90 mA amplitude, at 60, 90, and 120 Hz. Force measurements were collected and analyzed using LabVIEW 2012 (National Instruments).

Structure

Immediately after force testing, constructs were coated in Tissue Freezing Medium (Cat. No. 15-183-13; Fisher Scientific) and quickly frozen in dry ice-chilled isopentane before being stored at −80°C until sectioning. Ten micrometers cross-sectional and longitudinal samples of the SMUs were cryosectioned for structural analysis and gross morphology. Before immunostaining, the slides were fixed in −20°C methanol. Muscle structure was analyzed through immunohistochemical staining with antibodies for myosin heavy chain (MF20) (Cat. No. MF 20-c; DSHB), and laminin (Cat. No. 7463; Abcam). Hematoxylin and eosin (H&E) and Masson's trichrome staining were also completed to provide a qualitative assessment of overall structure.

Statistics

For all graphs, bars indicate mean ± standard deviation. Differences between groups were assessed with one-way ANOVA with *post hoc* multiple comparisons test. Significance was established at $p < 0.05$. Evaluations of histological samples of 3D constructs were solely qualitative.

Results

Digestion efficiency

Comparing the mass of undigested tissue and the cell yields of each muscle group provided insight into the digestion efficiency of each type of muscle. This characteristic is important to consider when assessing the clinical relevance of each muscle group as a source of primary cells. Comparisons of the mass of undigested tissue showed a significant difference between groups ($p < 0.0001$, $n = 14$ for zygomaticus major (ZM), $n = 16$ for others). The *post hoc* multiple comparisons test showed that all groups were significantly different from each other, with the zygomaticus major having the least efficient digestion (largest amount of undigested tissue) and the SM having the most efficient digestion (Fig. 2A). This same level of significance was not as apparent for the cell yield per mass of muscle digested, although there was a significant difference between groups ($p = 0.0313$, $n = 10$ for each group) (Fig. 2B). The masseter muscle yielded the largest number of cells per unit mass of muscle digested, but this was only significantly different from the ZM, which yielded the fewest cells ($p = 0.0278$). Taking these two metrics into consideration, overall, the ZM had the least efficient digestion, making it the least promising cell source in regard to cell yield.

Characterization of starting cell populations

We immunocytochemically stained aliquots of the muscle isolates to evaluate the starting cell populations of each muscle group. We co-stained for Pax7 and MyoD to identify myogenic cells and found that there was no significant difference in the number of myogenic cells between groups ($p = 0.7525$, $n = 2$ for soleus and $n = 4$ for others) (Fig. 3A). All groups had an average myogenic cell population between 5% and 10% of the total isolated cells, with the soleus having the lowest percentage on average and the SM having the highest. Specifically, the percentage of myogenic cells was $9.18\% \pm 2.74\%$, $7.63\% \pm 3.54\%$, $6.47\% \pm 2.06\%$, and

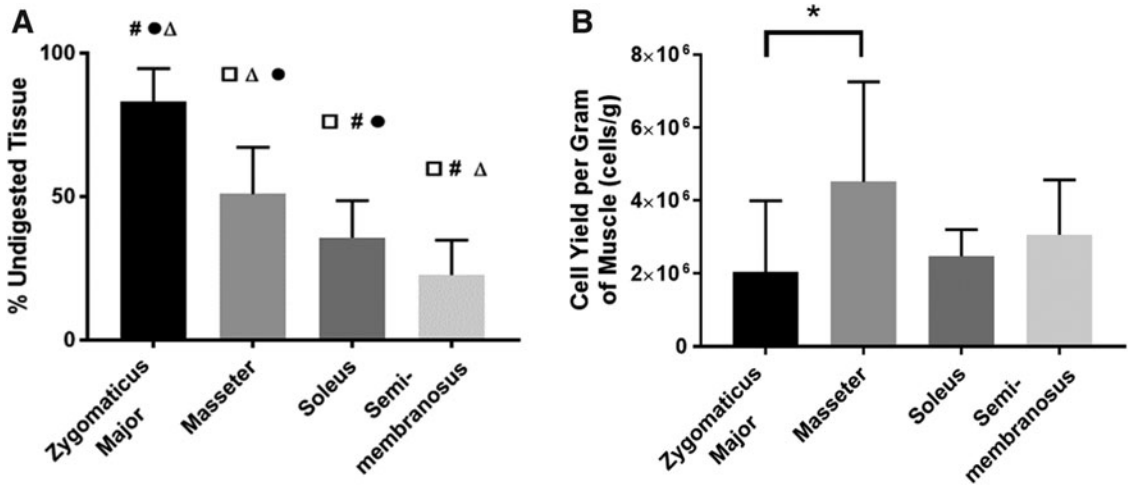

FIG. 2. Tissue digestion efficiency. **(A)** After allowing the tissue to enzymatically digest for 2.25 h, the undigested tissue was filtered out and weighed to provide insight into the digestion efficiency of each muscle group. There was a statistically significant difference in digestion efficiency between groups ($p < 0.0001$, $n = 14$ for ZM and $n = 16$ for others), and all groups were significantly different from each other. *Symbols* indicate statistically significant differences: □ from zygomaticus major, # from masseter, Δ from soleus, and ● from SM. **(B)** Upon completion of enzymatic digestion, cell counts were taken and normalized to the mass of muscle digested. There was a statistically significant difference in cell yield between groups ($p = 0.0313$, $n = 10$ for each group). The masseter yielded a significantly higher number of cells than the ZM ($p = 0.0278$). *$p < 0.05$. ZM, zygomaticus major.

9.50% ± 3.59% for the ZM, masseter, soleus, and SM, respectively. We also stained for vimentin to identify mesenchymal cells, including fibroblasts. The vimentin-positive cells made up ~30–40% of the total cell population. Again, there was no significant difference in the number of vimentin-positive cells between groups ($p = 0.5596$, $n = 2$ for soleus, $n = 3$ for SM, and $n = 4$ for others) (Fig. 3B). Specifically, the percentage of vimentin-positive cells was 40.83% ± 7.57%, 34.13% ± 10.90%, 32.59% ± 6.84%, and 30.78% ± 3.59% for the ZM, masseter, soleus, and SM,

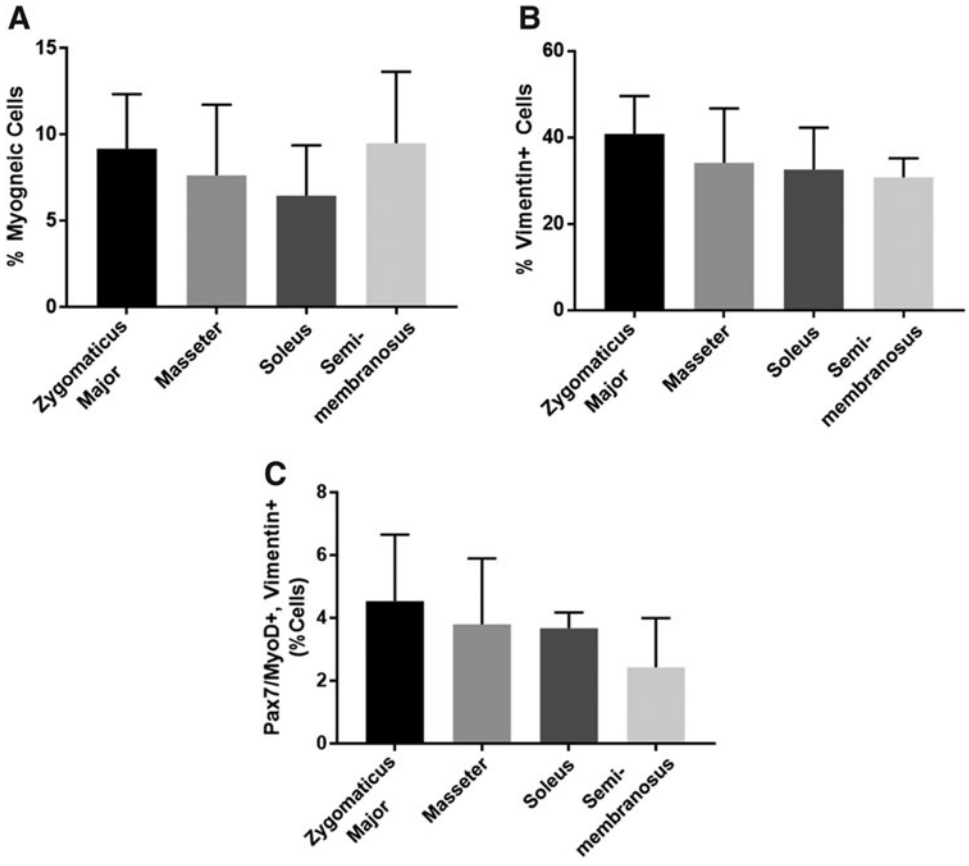

FIG. 3. Characterization of the isolated cell populations. The isolated cells were characterized to determine the percentage of **(A)** myogenic cells (expressing Pax7 and/or MyoD) and **(B)** mesenchymal cells (expressing vimentin), and **(C)** the number of cells expressing both Pax7/MyoD and vimentin present in the cell isolates. **(A)** There was no significant difference in the percentage of myogenic cells between groups ($p = 0.7525$, $n = 2$ for soleus and $n = 4$ for others). **(B)** There was no significant difference in the percentage of vimentin$^+$ cells between groups ($p = 0.5596$, $n = 2$ for soleus, $n = 3$ for SM, and $n = 4$ for others). **(C)** There was no significant difference in the percentage of cells expressing both Pax7/MyoD and vimentin between groups ($p = 0.4802$, $n = 2$ for soleus and $n = 4$ for others).

respectively. We also enumerated the percentage of cells expressing both Pax7/MyoD and vimentin and found that these values mirrored the trend seen in the percentage of vimentin-positive cells; however, there was no significant difference between groups ($p=0.4802$, $n=2$ for soleus and $n=4$ for others) (Fig. 3C).

Proliferative capacity and early differentiation

Comparing the proliferative capacities and early differentiation capabilities of the cells, we found that there were no significant difference in the number of $MyoD^+/mm^2$ cells between experimental groups, but there was a significant difference in $BrdU^+$ cells between groups ($p=0.0093$, $n=9$ for soleus and $n=11$ for others) (Fig. 4A). The SM plates had a significantly higher number of $BrdU^+$ cells/mm^2 than both the ZM ($p=0.0089$) and the masseter ($p=0.0037$) on day 4 (mean of 17.5 cells/mm^2 vs. 10.2 cells/mm^2 and 9.5 cells/mm^2, respectively). Immunostaining for myogenin was completed 6 days after initial plating. There was a statistically significant difference in the number of $myogenin^+$ cells/mm^2 between groups ($p=0.0292$, $n=10$ for ZM, $n=11$ for masseter, $n=12$ for soleus, and $n=13$ for SM), with the zygomaticus major having a statistically higher number of $myogenin^+$ cells/mm^2 than the masseter (mean of 616.5 cells/mm^2 vs. 364.1 cells/mm^2, $p=0.0326$) (Fig. 4B). While the SM had more proliferating $BrdU^+$ cells/mm^2 than the masseter and ZM, these cells were not necessarily myogenic cells, or at least were not expressing MyoD at this time point. The ZM, soleus, and SM showed no difference in the number of $myogenin^+$ cells/mm^2 on day 6, but the ZM did express a significantly higher number of cells than the masseter. However, this trend was not reflected in assays performed at later time points (i.e., myotube size and density and force production).

Late differentiation

Measures of myotube size and density revealed that there were significant differences between groups in both myotube size (diameter) and density (number of myotubes/mm^2) on day 11 (Fig. 5). These results are further reflected in the representative images of the developing monolayers (Fig. 5A–D). As can be noted from the images, the monolayer fabricated from zygomaticus major-derived cells appears to have a less dense myotube network and more fibroblast overgrowth compared to the other groups. Images such as these were used to evaluate myotube size and density on day 11. The masseter had significantly larger myotubes than the ZM ($p=0.0002$) and the SM ($p=0.0034$) (mean of 27.8 μm vs. 22.1 μm and 23.5 μm, respectively), and the soleus also had significantly larger myotubes than the ZM (mean of 25.5 μm vs. 22.1 μm, $p=0.0202$) (Fig. 5E). There was also a significant difference in the number of myotubes/mm^2 between groups: the SM had significantly more myotubes/mm^2 than the ZM ($p=0.0029$), soleus ($p=0.0055$), and masseter ($p=0.0007$) (mean of 32.3 myotubes/mm^2 vs. 25.5, 26.0, and 24.4 myotubes/mm^2, respectively) (Fig. 5F).

Function

After formation of the 3D construct, measures of maximum tetanic force production were taken to assess the SMUs' functionality (Fig. 6). An ordinary one-way ANOVA revealed that there was a significant difference in force production between groups ($p=0.0156$, $n=22$ for ZM, $n=25$ for masseter, $n=26$ for soleus, and $n=25$ for SM). A *post hoc* multiple comparisons

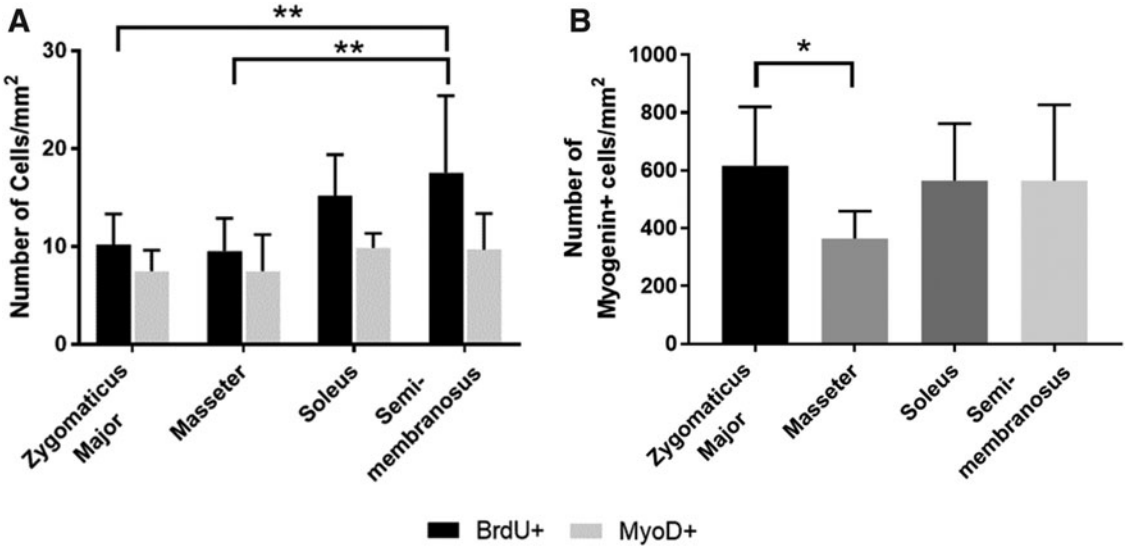

FIG. 4. Myogenic proliferation and early differentiation. **(A)** A BrdU assay coupled with immunostaining for MyoD was completed 4 days after initial plating. There were no significant differences in the number of $MyoD^+/mm^2$ cells between groups, but there was a significant difference in $BrdU^+$ cells between groups ($p=0.0093$, $n=9$ for soleus and $n=11$ for others). The SM plates had a significantly higher number of $BrdU^+$ cells/mm^2 than both the zygomaticus major ($p=0.0089$) and the masseter ($p=0.0037$) on day 4. **(B)** Immunostaining for myogenin completed 6 days after initial plating. There was a statistically significant difference in the number of $myogenin^+$ cells/mm^2 between groups ($p=0.0292$, $n=10$ for ZM, $n=11$ for masseter, $n=12$ for soleus, and $n=13$ for SM), with the zygomaticus major having a statistically higher number of $myogenin^+$ cells/mm^2 than the masseter ($p=0.0326$). $^*p<0.05$, $^{**}p<0.01$.

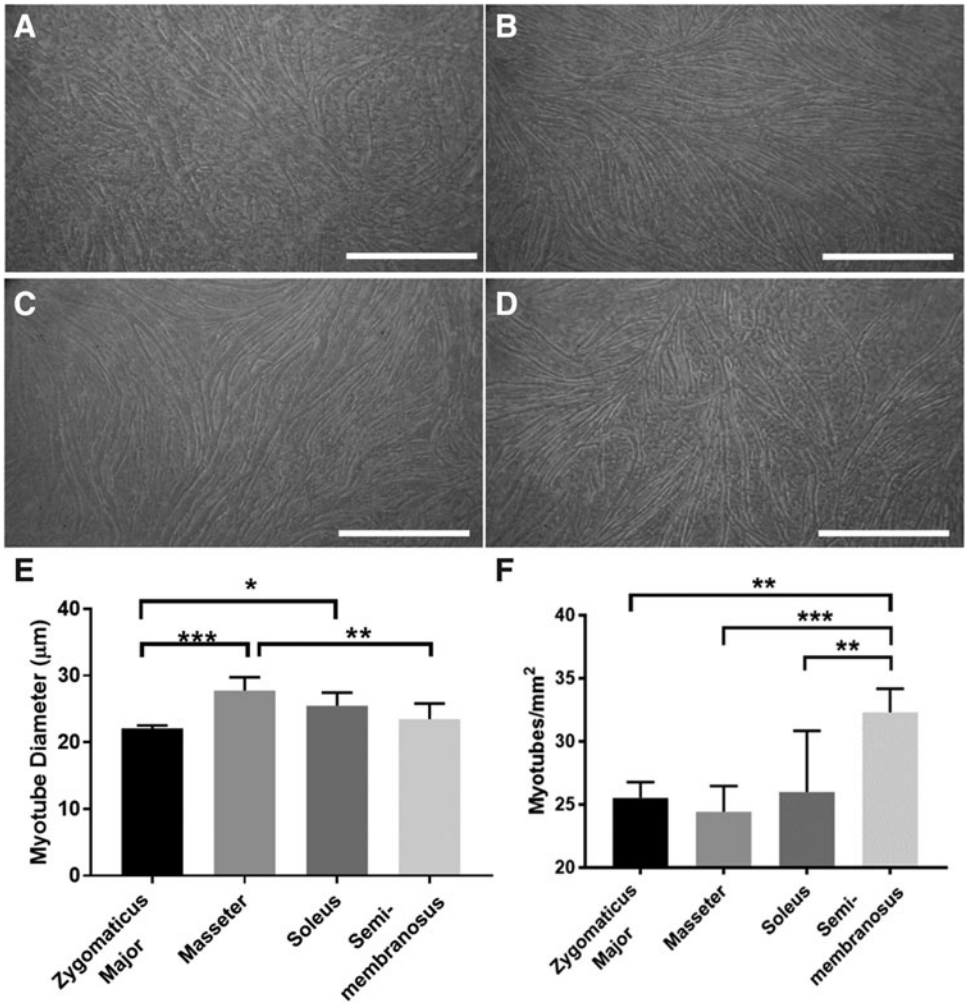

FIG. 5. Late differentiation. Light microscopy images of the monolayers were taken before 3D construct formation to visualize the development of the myotubes. The images depicted show representative 10× images of monolayers fabricated from **(A)** zygomaticus major, **(B)** masseter, **(C)** soleus, and **(D)** SM muscle sources. As can be noted from the images, the zygomaticus major group exhibited a less dense myotube network and more fibroblast overgrowth compared to the other groups. Scale bars = 500 μm. **(E, F)** Images such as these were used to evaluate myotube size (diameter) and density (number of myotubes/mm^2) on day 11. **(E)** There was a significant difference in myotube size between groups ($p = 0.0002$, $n = 6$ for each group). The masseter had significantly larger myotubes than the ZM ($p = 0.0002$) and the SM ($p = 0.0034$). The soleus also had significantly larger myotubes than the ZM ($p = 0.0202$). **(F)** There was also a significant difference in the number of myotubes/mm^2 between groups ($p = 0.0005$, $n = 6$ for each group). The SM had significantly more myotubes/mm^2 than the ZM ($p = 0.0029$), soleus ($p = 0.0055$), and masseter ($p = 0.0007$). *$p < 0.05$, **$p < 0.01$, ***$p < 0.001$.

test revealed that SMUs fabricated from masseter muscle produced significantly higher forces than those fabricated from the zygomaticus major (mean of 61.7 μN vs. 10.4 μN, $p = 0.0110$). However, there were no significant differences in force production between SMUs fabricated from the masseter, soleus, or SM muscles. Out of these three groups, the SMUs fabricated from the masseter muscle experienced the highest standard deviation, indicating high SMU variability within this group.

Structure

Cross-sections of 3D constructs provided some insight into the composition of the SMUs. Masson's trichrome staining of SMU cross-sections revealed similarly abundant collagen deposition in all groups (Fig. 7A–D). The collagen deposition is important in that it contributes to the structural integrity of the constructs. In the immunohistochemistry (IHC) staining, laminin costained with myosin heavy chain (MF20) similarly to the way the basal lamina surrounds each muscle fiber in native muscle tissue (Fig. 7E–H). Qualitatively, compared to the other muscle sources, the SMUs fabricated from ZM appeared to have less MF20 staining relative to the number of nuclei in the construct (Fig. 7I–L). This hypercellularity compared to the other groups was noted in all stains. Furthermore, SMUs fabricated from ZM had less-organized laminin protein. The combination of hypercellularity of MF20-negative cells and less organized laminin likely contributed to the decreased force production of that group. In addition, the masseter and soleus groups appeared to have more evenly dispersed MF20 staining.

Staining of longitudinal sections of 3D constructs was conducted to determine the degree of structural organization

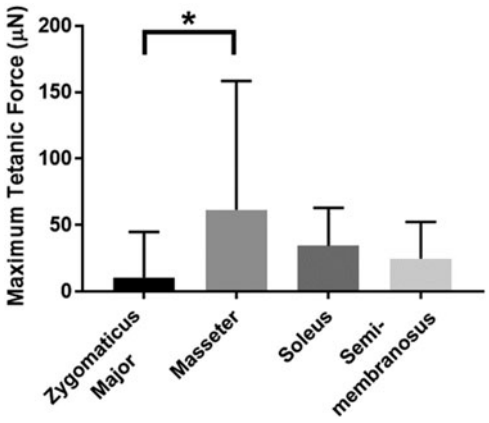

FIG. 6. Maximum tetanic force production. Isometric force production in response to a tetanic electrical stimulus was measured 24 h after 3D construct formation. There was a significant difference in force production between groups ($p = 0.0156$, $n = 22$ for zygomaticus major, $n = 26$ for soleus, and $n = 25$ for others). The SMUs fabricated from masseter produced significantly more force than those fabricated from the zygomaticus major ($p = 0.0110$). *$p < 0.05$.

and anisotropy of each group (data not shown). The hypercellularity of constructs from the ZM groups was also noted in these H&E and IHC stains. MF20 and laminin staining revealed myotube-like structures oriented longitudinally throughout the constructs in all groups; however, there appeared to be a lower degree of alignment present in the ZM group compared to the other groups, which were relatively equivalent in their alignment. This observation may explain why the ZM group had the lowest average force production, as a high degree of myotube alignment is important to maximize the force production capabilities of the constructs. In addition, nuclei were present throughout the entire thickness of the construct in all groups. Because the constructs were not fully fused, we believe this characteristic helped prevent the formation of a necrotic core.

Discussion

Overall, this study aimed to evaluate both craniofacial and hindlimb muscles as the source of muscle-derived progenitor cells for the fabrication of tissue-engineered skeletal muscle. Inhomogeneity of cells, especially satellite cells, between craniofacial and limb sources has been well documented in the literature.[12–16] In this study, we sought to evaluate myogenic potential of cells derived from the ovine zygomaticus major, masseter, soleus, and SM muscles throughout the SMU fabrication process.

It is important to keep translatability and clinical relevance in mind when designing engineered tissue. In general, when starting with a fresh tissue biopsy as a cell source, yielding the greatest number of muscle progenitor cells possible from the smallest biopsy is of utmost importance in terms of economic efficiency and reducing the potential for donor site morbidity from a live biopsy. While the masseter muscle yielded the most cells per unit mass of muscle digested, this value was not significantly different from the cell yield for the soleus or the SM. Overall, the ZM had the poorest digestion efficiency, with the largest amount of undigested tissue and the lowest overall cell yield. Use of the ZM as a muscle source would require much larger biopsies, making it more costly and more inconvenient,

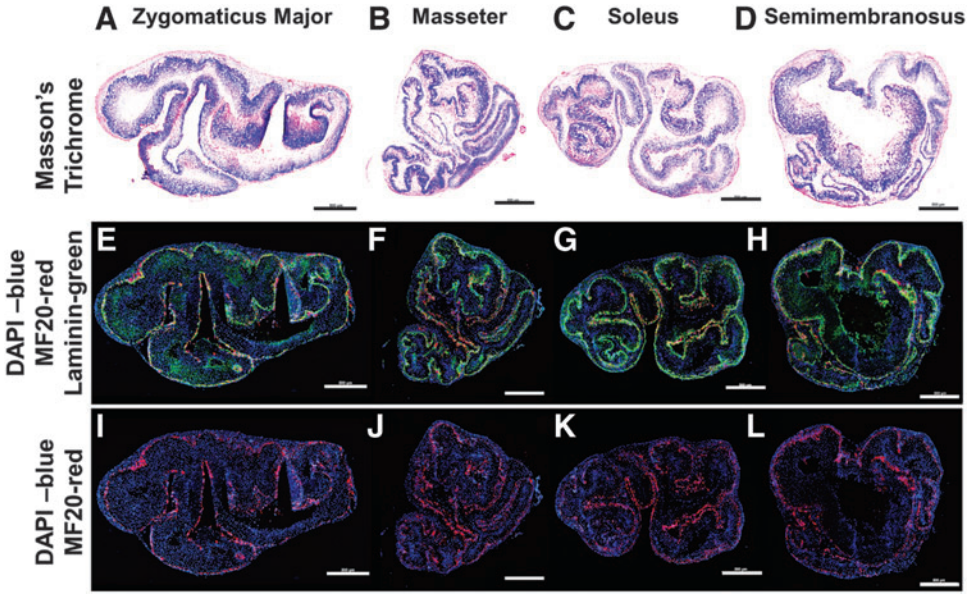

FIG. 7. Visualization of myotubes within 3D SMUs. Histology was conducted on cross-sections of the three-dimensional constructs. The images depicted show representative images of SMUs fabricated from **(A, E, I)** zygomaticus major, **(B, F, J)** masseter, **(C, G, K)** soleus, and **(D, H, L)** SM muscle sources. Masson's trichrome **(A–D)** was performed to visualize collagen (*blue*), as well as muscle (*red*) and other cellular material (*red*). IHC **(E–L)** was performed to visualize the presence of laminin protein (*green*), muscle fibers (MF20, *red*), and cell nuclei (DAPI, *blue*). As can be noted from the images, the SMU fabricated from the zygomaticus major appeared to exhibit hypercellularity and less defined laminin staining compared to the other groups. Scale bars = 500 μm.

especially considering the small size of the muscle. The fact that the ZM was more difficult to digest and yielded fewer cells is potentially due to the involvement of the superficial musculoaponeurotic system (SMAS), which is described as a fibrous connective tissue network that integrates with facial muscles to amplify their activity in facial expression. With regard to the ZM, the SMAS is described as horizontal fibrous connective tissues that envelop the zygomaticus musculature.[31,32] This could explain the large amounts of connective tissue observed during the cell isolation process, as well as the poor digestion efficiency of the ZM overall.

While we did observe a significant difference in the overall number of cells harvested during digestion of the tissue, we did not observe a significant difference in the percentage of myogenic cells yielded between muscle groups. In all muscles tested, the average percentage of myogenic cells yielded was $\sim$5–10% of the total cells. We expected the myogenic cell composition to correlate with the fiber type of the muscle; specifically, we expected the muscles with a higher percentage of type I fibers to yield a greater percentage of satellite cells, as described in the literature.[27] However, our data did not support this and was characterized by variability within groups. Each data point represented an individual animal, so this variability could be attributed to variation between animals.

Individual variability, including the effects of sex, age, and castration on skeletal maturity, muscle fiber type composition, and satellite cell density are well documented in the literature[24,33–40]; however, the effects vary across species. For example, in mice, the decrease in satellite cells that occurs with age is dependent on fiber type,[37,38] while this decrease in satellite cells with age has not been noted in type I fibers in humans.[40] In sheep, Cancellara *et al.* found that age has a significant effect on the fiber type composition of muscles, as well as the gene expression.[33] They found that the fiber type composition of the masseter progressively switches to a slow phenotype, while the SM progressively switches to fast phenotype over the course of the first 6 months of age.[33] This variability between animals was also noted in ZM fiber type composition data that were collected as part of an unrelated study. We found that type II fibers made up $54.35\% \pm 11.07\%$ of the fibers, with 3 out of 11 animals having a type II fiber composition of less than 50%. This contrasts with a study by Schwarting *et al.*, which collected data on four humans and found the ZM to have a type I fiber composition of 66%.[26] A similar level of individual variability may have been present in the other muscle groups, which could explain the differences in the percentage of myogenic cells within muscle groups.

These studies support the idea that many factors could have contributed to the variability noted within groups and could have potentially affected myogenic cell yield and quality. This is especially true for the characterization of the starting cell population because we did not control for sex, age, or breed of the animals used in this assay. In all other assays, the cells used came from animals that were the same sex and breed, and were within 3 months of age of each other.

Measures of myogenic proliferation showed that all groups were statistically equivalent on day 4. While the SM group demonstrated the highest overall proliferative capacity, this value was not significantly different from the soleus group. Measures of early myogenic differentiation revealed that the ZM, soleus, and SM groups were not significantly different, and the masseter had significantly fewer myogenin$^+$ cells/mm^2 than the ZM on day 6. There was a large difference between the number of cells that were BrdU positive or MyoD positive on day 4 and the number of cells that were myogenin positive on day 6. We believe this difference can be attributed to several factors. First, on day 4, the total cell count was roughly 100 cells/mm^2, whereas only $\sim$5–15% of cells were expressing BrdU or MyoD at this time point. In contrast, on day 6, the total cell count was roughly 1500 cells/mm^2 and the cells expressing myogenin usually made up $\sim$25–35% of the total cells. It is worth noting that there are several cell types on the plates, each with different growth rates. Second, another reason the growth rates may have been so high between days 4 and 6 is that the cells are fed for the first time on day 4. During the feeding, much of the debris from the initial isolation is removed. We believe the presence of isolation debris may inhibit cell growth, and its removal on day 4 may accelerate the proliferation rate. The plates used for the BrdU/MyoD assay were fixed and stained before the first feeding, which may contribute to the difference in total cell number.

Furthermore, differences in the differentiation timelines of cell populations from different muscle sources have been noted in the literature,[12–14] and it is possible that the time points that were evaluated in this study did not demonstrate the optimal time point for that muscle source, especially with regard to the expression of molecular myogenic markers. For example, Ono *et al.* found that mouse satellite cells derived from the masseter muscle ''proliferate more and differentiate later than those from limb muscles.''[14] Our data support this observation; we found that the masseter had the lowest average number of myogenin$^+$ cells/mm^2 on day 6. Thus, data collected from time points later in the fabrication process (i.e., myotube size and density and force production, and histology) are more relevant for comparing groups.

Later time points in the fabrication process showed that monolayers fabricated from SM-derived cells had significantly more myotubes/mm^2 than all other groups, with the average number of myotubes/mm^2 being 24–32% higher than the other groups. However, these myotubes were not necessarily as large in diameter as those in other groups. In terms of functionality, forces produced by constructs fabricated from the masseter, soleus, and SM muscles were statistically equivalent. However, the forces in the masseter group had a high level of variability. This variability could be attributed to differences in individual animal donors. Histological findings supported force production data; SMUs in the ZM group were characterized by hypercellularity, less defined laminin staining, and reduced MF20 staining, as well as less aligned myotubes. All of these factors would have translated to reduced force production. Notably, no qualitative histological differences between SMUs from the other groups were observed.

Ultimately, while this study did not clearly reveal an optimal cell source, what is clear from the results is that the ZM is the least suitable source for harvesting muscle-derived progenitor cells. The ZM group also experienced the least efficient digestion, the lowest average force production, and histologically, the least aligned myosin heavy

chain staining. With regard to the size of the muscle, there is also low tissue availability, making it less clinically relevant, although the small muscle size is also true for the masseter muscle. For the most part, the soleus performed on par with the SM group, with the exception of myotube density. However, the soleus is less clinically relevant than the SM because it is not a superficial muscle and biopsies would be more invasive. Overall, the SM is the muscle that seems to be best suited as a cell source for muscle-derived cells, although the soleus is also well suited.

Acknowledgments

The authors would like to acknowledge Alejandro Moncada for his technical assistance.

Disclosure Statement

No competing financial interests exist.

Funding Information

This research was supported by National Institutes of Health/National Institute of Arthritis and Musculoskeletal and Skin Diseases (1R01AR067744-01) and the National Institutes of Health Research Supplement to Promote Diversity in Health-Related Research (3R01AR067744-02W1).

References

1. American Society of Plastic Surgeons. 2017 National Plastic Surgery Statistics. Illinois: American Society of Plastic Surgeons, 2017.
2. Lew, T.A., Walker, J.A., Wenke, J.C., Blackbourne, L.H., and Hale, R.G. Characterization of craniomaxillofacial battle injuries sustained by United States service members in the current conflicts of Iraq and Afghanistan. J Oral Maxillofac Surg **68,** 3, 2010.
3. Gassner, R., Tuli, T., Hächl, O., Rudisch, A., and Ulmer, H. Cranio-maxillofacial trauma: a 10 year review of 9,543 cases with 21,067 injuries. J Craniomaxillofac Surg **31,** 51, 2003.
4. Carlson, B.M., and Faulkner, J.A. The regeneration of skeletal muscle fibers following injury: a review. Med Sci Sports Exerc **15,** 187, 1983.
5. Carlson, B.M. Regeneration of the completely excised gastrocnemius muscle in the frog and rat from minced muscle fragments. J Morphol **125,** 447, 1968.
6. Mase, V.J., Hsu, J.R., Wolf, S.E., *et al.* Clinical application of an acellular biologic scaffold for surgical repair of a large, traumatic quadriceps femoris muscle defect. Orthopedics **33,** 511, 2010.
7. Mao, J.J., Stosich, M.S., Moioli, E.K., *et al.* Facial reconstruction by biosurgery: cell transplantation versus cell homing. Tissue Eng Part B Rev **16,** 257, 2010.
8. Mertens, J.P., Sugg, K.B., Lee, J.D., and Larkin, L.M. Engineering muscle constructs for the creation of functional engineered musculoskeletal tissue. Regen Med **9,** 89, 2014.
9. Leckenby, J., and Grobbelaar, A. Smile restoration for permanent facial paralysis. Arch Plast Surg **40,** 633, 2013.
10. VanDusen, K.W., Syverud, B.C., Williams, M.L., Lee, J.D., and Larkin, L.M. Engineered skeletal muscle units for repair of volumetric muscle loss in the tibialis anterior muscle of a rat. Tissue Eng Part A **20,** 2920, 2014.
11. Sicari, B.M., Dearth, C.L., and Badylak, S.F. Tissue engineering and regenerative medicine approaches to enhance the functional response to skeletal muscle injury. Anat Rec (Hoboken) **297,** 51, 2014.
12. Harel, I., Nathan, E., Tirosh-Finkel, L., *et al.* Distinct origins and genetic programs of head muscle satellite cells. Dev Cell **16,** 822, 2009.
13. Pavlath, G.K., Thaloor, D., Rando, T.A., Cheong, M., English, A.W., and Zheng, B. Heterogeneity among muscle precursor cells in adult skeletal muscles with differing regenerative capacities. Dev Dyn **212,** 495, 1998.
14. Ono, Y., Boldrin, L., Knopp, P., Morgan, J.E., and Zammit, P.S. Muscle satellite cells are a functionally heterogeneous population in both somite-derived and branchiomeric muscles. Dev Biol **337,** 29, 2010.
15. Michailovici, I., Eigler, T., and Tzahor, E. Craniofacial muscle development. Curr Top Dev Biol **115,** 3, 2015.
16. Collins, C.A., Olsen, I., Zammit, P.S., *et al.* Stem cell function, self-renewal, and behavioral heterogeneity of cells from the adult muscle satellite cell niche. Cell **122,** 289, 2005.
17. Syverud, B.C., VanDusen, K.W., and Larkin, LM. Effects of dexamethasone on satellite cells and tissue engineered skeletal muscle units. Tissue Eng Part A **22,** 480, 2016.
18. Williams, M.L., Kostrominova, T.Y., Arruda, E.M., and Larkin, L.M. Effect of implantation on engineered skeletal muscle constructs. J Tissue Eng Regen Med **7,** 434, 2013.
19. Gollnick, P.D., Sjödin, B., Karlsson, J., Jansson, E., and Saltin, B. Human soleus muscle: a comparison of fiber composition and enzyme activities with other leg muscles. Pflugers Arch **348,** 247, 1974.
20. Dodson, M.V., Mathison, B.A., and Mathison, B.D. Effects of medium and substratum on ovine satellite cell attachment, proliferation and differentiation in vitro. Cell Differ Dev **29,** 59, 1990.
21. Dodson, M.V., McFarland, D.C., Martin, E.L., and Brannon, M.A. Isolation of Satellite Cells from Ovine Skeletal Muscles. J Tissue Cult Methods **10,** 233, 1986.
22. Burton, N.M., Vierck, J., Krabbenhoft, L., Bryne, K., and Dodson, M.V. Methods for animal satellite cell culture under a variety of conditions. Methods Cell Sci **22,** 51, 2000.
23. Garrett, W.E., Califf, J.C., and Bassett, F.H. Histochemical correlates of hamstring injuries. Am J Sports Med **12,** 98, 1984.
24. Osterlund, C., Thornell, L.E., and Eriksson, P.O. Differences in fibre type composition between human masseter and biceps muscles in young and adults reveal unique masseter fibre type growth pattern. Anat Rec (Hoboken) **294,** 1158, 2011.
25. Stål, P. Characterization of human oro-facial and masticatory muscles with respect to fibre types, myosins and capillaries. Morphological, enzyme-histochemical, immunohistochemical and biochemical investigations. Swed Dent J Suppl **98,** 1, 1994.
26. Schwarting, S., Schröder, M., Stennert, E., and Goebel, H.H. Enzyme histochemical and histographic data on normal human facial muscles. ORL J Otorhinolaryngol Relat Spec **44,** 51, 1982.
27. Hawke, T.J., and Garry, D.J. Myogenic satellite cells: physiology to molecular biology. J Appl Physiol (1985) **91,** 534, 2001.
28. Committee for the Update of the Guide for the Care and Use of Laboratory Animals. Guide for the Care and use of Laboratory Animals. Washington D.C.: National Academies Press, 2010.

29. Syverud, B.C., Lee, J.D., VanDusen, K.W., and Larkin, L.M. Isolation and purification of satellite cells for skeletal muscle tissue engineering. J Regen Med **3,** 117, 2014.
30. Dennis, R.G., and Kosnik, P.E. Excitability and isometric contractile properties of mammalian skeletal muscle constructs engineered in vitro. In Vitro Cell Dev Biol Anim **36,** 327, 2000.
31. Hwang, K., and Choi, J.H. Superficial fascia in the cheek and the superficial musculoaponeurotic system. J Craniofac Surg **29,** 1378, 2018.
32. Broughton, M., and Fyfe, G.M. The superficial musculoaponeurotic system of the face: a model explored. Anat Res Int **2013,** 794682, 2013.
33. Cancellara, L., Quartesan, S., Toniolo, L., *et al.* Age-dependent variations in the expression of myosin isoforms and myogenic factors during the involution of the proximal sesamoidean ligament of sheep. Res Vet Sci **124,** 270, 2019.
34. Popkin, P.R.W., Baker, P., Worley, F., Payne, S., and Hammon, A. The Sheep Project (1): determining skeletal growth, timing of epiphyseal fusion and morphometric variation in unimproved Shetland sheep of known age, sex, castration status and nutrition. J Archaeol Sci **39,** 1775, 2012.
35. Melotti, L., Vezzoli, E., Mascarello, F., Maccatrozzo, L., and Patruno, M. The natural involution of the sheep proximal sesamoidean ligament is due to depletion of satellite cells and simultaneous proliferation of fibroblasts: ultrastructural evidence. Res Vet Sci **124,** 106, 2019.
36. McCormick, R., and Vasilaki A. Age-related changes in skeletal muscle: changes to life-style as a therapy. Biogerontology **19,** 519, 2018.
37. Day, K., Shefer, G., Shearer, A., and Yablonka-Reuveni, Z. The depletion of skeletal muscle satellite cells with age is concomitant with reduced capacity of single progenitors to produce reserve progeny. Dev Biol **340,** 330, 2010.
38. Chakkalakal, J.V., Jones, K.M., Basson, M.A., and Brack, A.S. The aged niche disrupts muscle stem cell quiescence. Nature **490,** 355, 2012.
39. Shefer, G., Van de Mark, D.P., Richardson, J.B., and Yablonka-Reuveni, Z. Satellite-cell pool size does matter: defining the myogenic potency of aging skeletal muscle. Dev Biol **294,** 50, 2006.
40. Verdijk, L.B., Snijders, T., Drost, M., Delhaas, T., Kadi, F., and van Loon, L.J. Satellite cells in human skeletal muscle; from birth to old age. Age (Dordr) **36,** 545, 2014.

Address correspondence to:
Lisa M. Larkin, PhD
Department of Molecular and Integrative Physiology
Biomedical Engineering
University of Michigan
Biomedical Science Research Building (BSRB)
109 Zina Pitcher Place Room #2025
Ann Arbor, MI 48109-2200

E-mail: llarkin@umich.edu

Received: March 27, 2019
Accepted: August 27, 2019
Online Publication Date: October 8, 2019